# Koopman Approximator based Adaptive Model Predictive Control of Continuous Nonlinear Systems

Yi Zheng[1], Yueyan Zhang[2], Qiangyu Li[1], Shaoyuan Li[1], and Min Luo[1]

[1]Affiliation not available
[2]Shanghai Jiao Tong University

September 30, 2022

**Abstract**

This paper considers the real-time control of a class of complex continuous nonlinear systems with an increasing requirement on control accuracy and unknown dynamics at the start time due to their complex dynamics and uncertainties. A Koopman approximate model-based adaptive MPC design using the Lyapunov technique is explored. Specifically, the nonlinear system is modeled/transformed into a linear model in a lifting space with the Koopman operator. A recursive update of the approximator is provided by which the parameters set of the approximator is in a nested form and a shrinking of the boundary of the approximator's mismatch from the real system is obtained. Also, based on the Koopman model and its mismatch boundary, a sufficient condition that ensures the states of the nonlinear system eventually converge to a small neighborhood of the origin is deduced. An FCCU example is employed to show the effectiveness of the proposed control law.

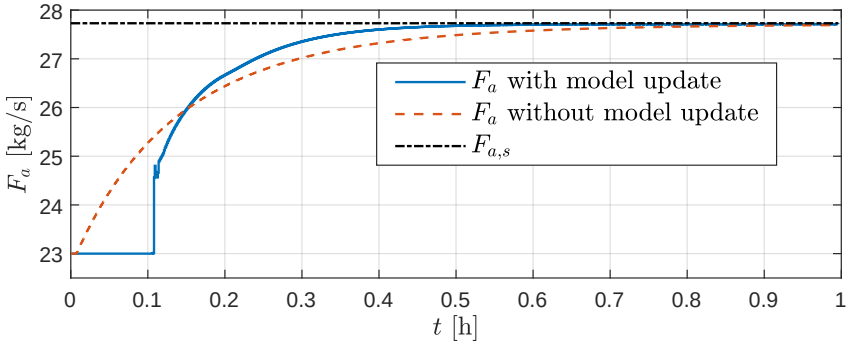

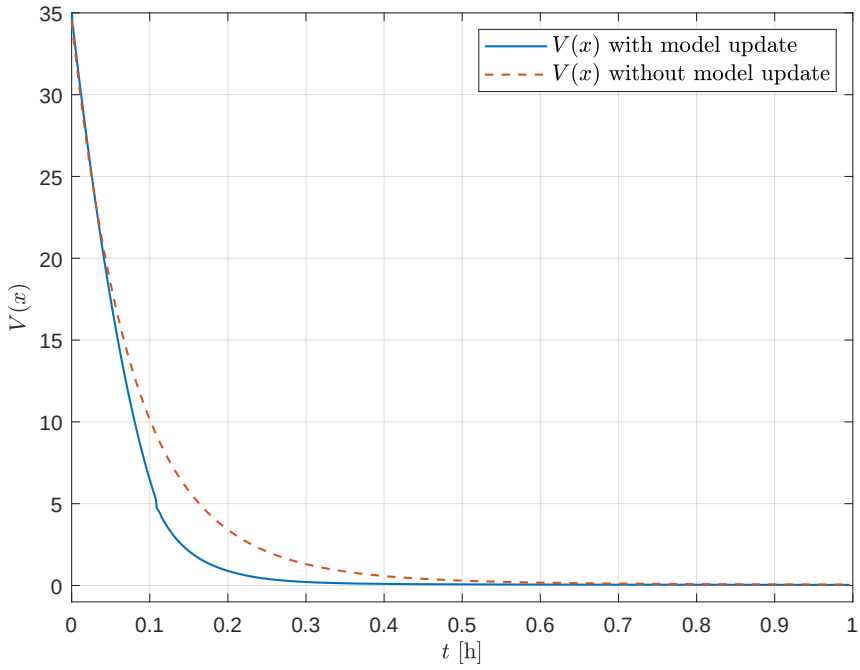

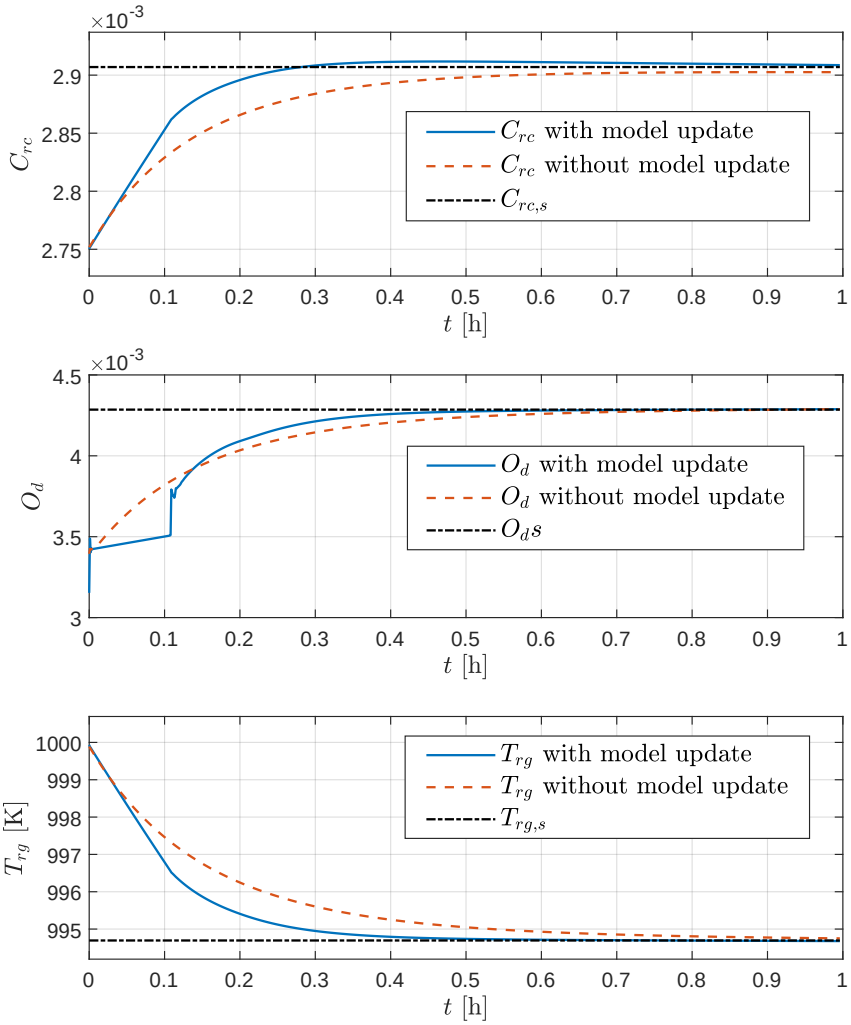

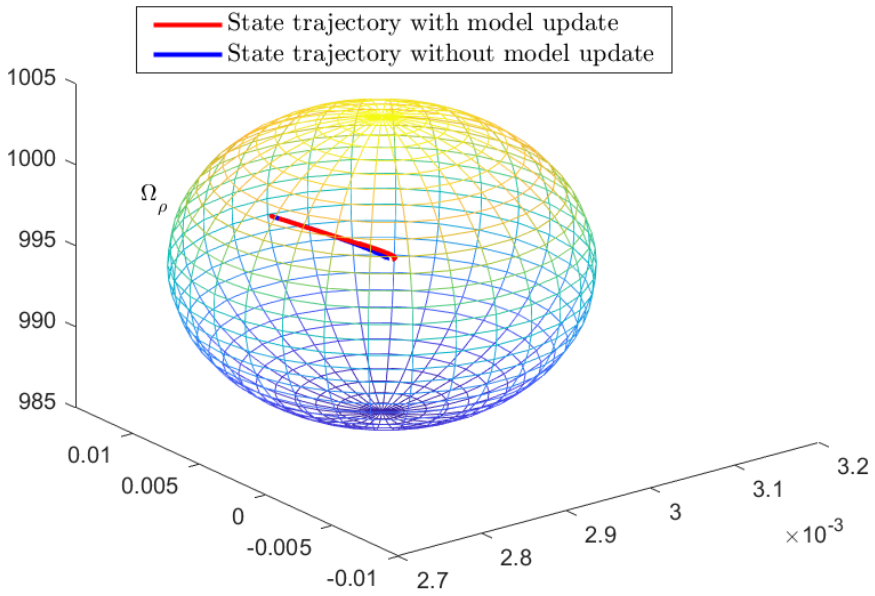


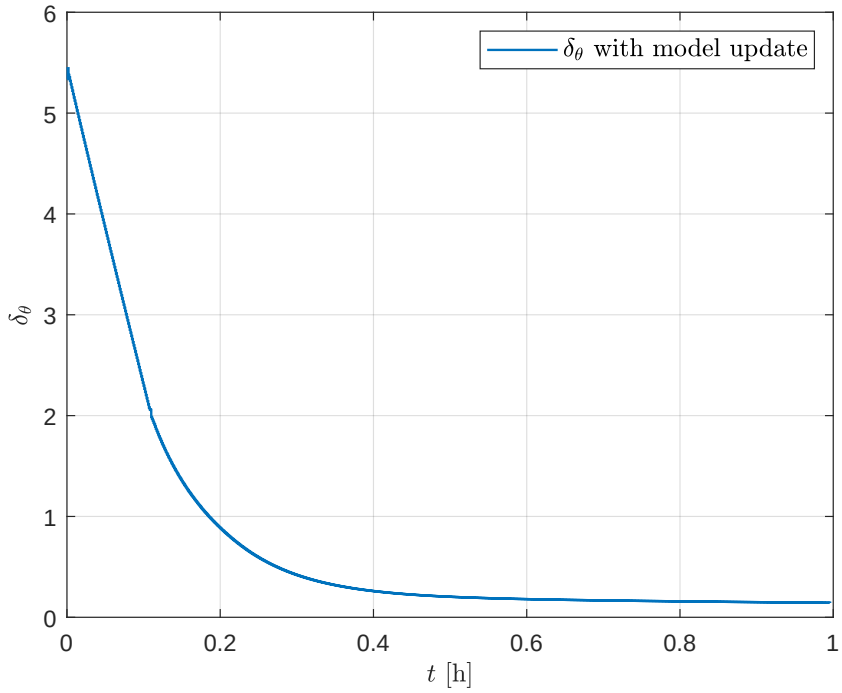

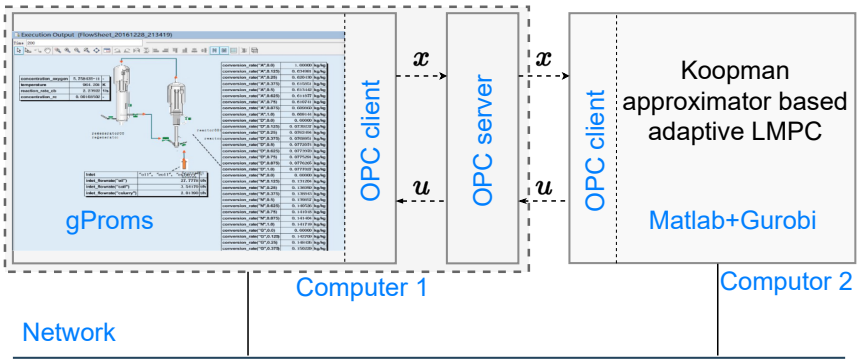


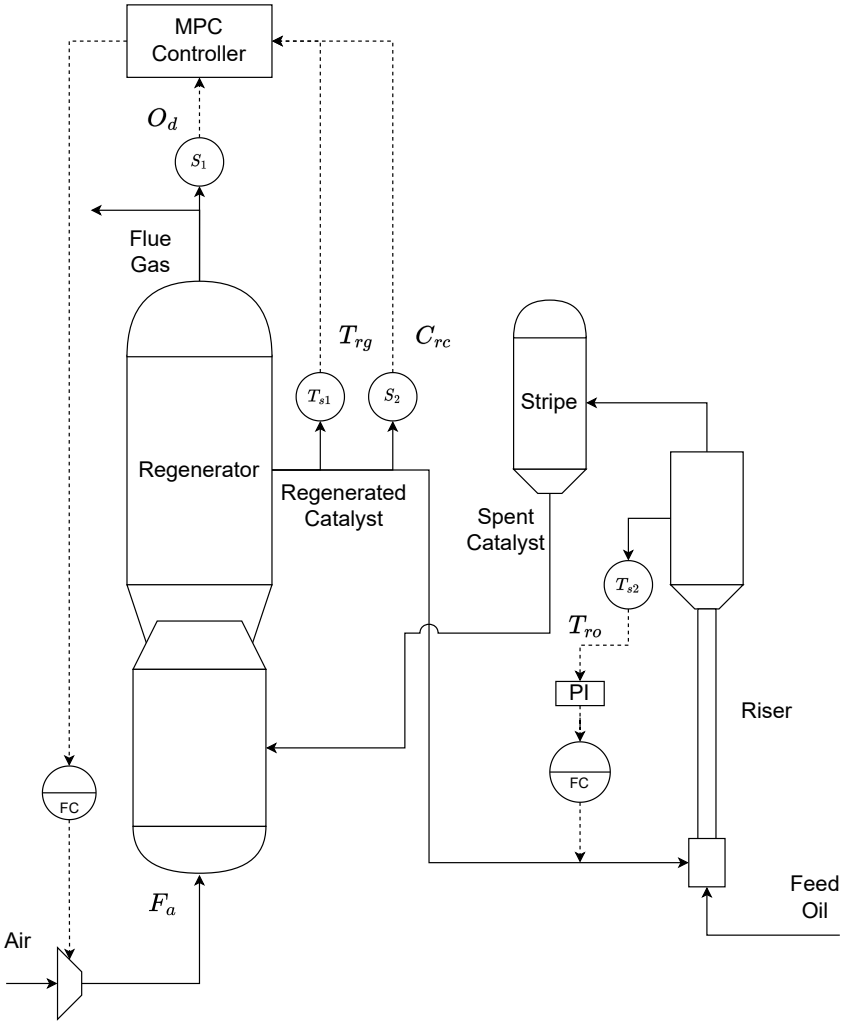

# Koopman Approximator based Adaptive Model Predictive Control of Continuous Nonlinear Systems

Yi Zheng, Yueyan Zhang, Qiangyu Li, Shaoyuan Li, Min Luo *

September 26, 2022

**Abstract**

This paper considers the real-time control of a class of complex continuous nonlinear systems with an increasing requirement on control accuracy and unknown dynamics at the start time due to their complex dynamics and uncertainties. A Koopman approximate model-based adaptive MPC design using the Lyapunov technique is explored. Specifically, the nonlinear system is modeled/transformed into a linear model in a lifting space with the Koopman operator. A recursive update of the approximator is provided by which the parameters set of the approximator is in a nested form and a shrinking of the boundary of the approximator's mismatch from the real system is obtained. Also, based on the Koopman model and its mismatch boundary, a sufficient condition that ensures the states of the nonlinear system eventually converge to a small neighborhood of the origin is deduced. The steady-state error of the MPC system keeps decreasing. By the proposed method, 1) the performance of the closed-loop system is expected to be improved due to the continuous improving predictive model accuracy, 2) efficient computational performance is obtained benefiting from the usage of the linear propriety of the Koopman operator, and 3) it is not necessary to assume the distribution of the system disturbance a prior. An FCCU example is employed to show the effectiveness of the proposed control law.

*Keywords:* Model Predictive Control; Lyapunov based control; nonlinear system; Adaptive control; Set-Membership identification

*Yi Zheng, Yueyan Zhang, Qiangyu Li, Shaoyuan Li, and Min Luo are with the Department of Automation, Shanghai Jiao Tong University, Key Laboratory of System Control and Information Processing, Ministry of Education of China, Shanghai 200240, China, Phone:+86-34208653. This work is supported by the National Nature Science Foundation of China (61673273,61590924), Corresponding author Y. Zheng, S. LI. Tel. +86 02134208653.

# 1 Introduction

With the rise of big data analytics, data-driven or machine learning methodologies have gained increasing recognition and demonstrated successful implementation in many traditional engineering fields. Nowadays, the modern chemical manufacturing process has become more and more complex and constantly accompanied by high non-linearity, slow time-varying dynamics due to unforeseen process changes or large external unmeasurable disturbances, equipment wearing, etc. During process operation, the model used to predict the future evolution of the system state may not always remain accurate as time progresses [1]. Even in the case where a deterministic first-principles model is developed based on fundamental understanding, there may be inherent simplifying assumptions involved. The plant model mismatch degrades the performance of the control algorithms, which is not expected for systems with requirements of high control precision.

Given these considerations, the data-driven or machine-learning-model-based control design has been a hot topic for obtaining the improvement of the performance of the model-based control system [1–8]. It efficiently incorporates the machine learning, and data analysis technologies into the online update of the system model [3, 8], then let the predictive model be consistent with the real process gradually. The learning-based Model Predictive Control (MPC) [3,4,8,9] is a typical method and has attracted much more attention. It not only has the virtues of machine-learning-based control mentioned above but also inherits the advantages of MPC, e.g, explicitly handling constraints, good optimization performance, and being recognized as a practical control method with wildly application fields.

Some methods appear in the literature for nonlinear systems. Ref. [3] proposed an LMPC taking Recurrent Neuro Network (RNN) as the predictive model, where the RNN updates before the stability condition is violated. Ref. [10] derived a generalization error bound via the Rademacher complexity method for RNN to establish closed-loop system stability properties. Ref. [11,12] and [7] proposed an MPC with an online updating Gaussian Process (GP) model. Among them, Ref [11] provided GP data set update rules by which the recursive feasibility and the stability of the MPC system are guaranteed in a certain probability. The conditions to update the system model are based on the estimation of model mismatch of GP at the current state. Ref. [4, 13] proposed Q-learning-based MPCs, where the actor-critic framework which includes a critic artificial neural network (NN) and an actor NN, are used in the implementation of the methods. Adaptive dynamic optimization is used to update the two NNs. With consideration that the nonlinear property of the machine-learning-based model, the solving of the MPC optimization problem, even the model update, becomes time-consuming for complex systems.

Since the mismatch between the predictive model and the real system in learning-based MPC

varied with the model updating, the guaranteeing of the stability and constraint satisfaction of the MPC system becomes a problem. One effective and conservative way to design stabilized MPC is based on the maximum boundary of model mismatch. It considers the worst case of model uncertainty and inaccuracy and may lead to poor performance. Ref. [14,15] proposed Lyapunov-based MPC where the asynchronous measurements and delays were explicitly taken into account. It assumed that there exist an upper bound on the interval between two consecutive asynchronous measurements and an upper bound on the maximum measurement delay. The method guarantees that the closed-loop state is always bounded in the predefined stability region and is ultimately bounded in a small region containing the origin. Ref. [16] proposed an event-triggered method, which considers a fixed error boundary, and triggered the model update when the state may exceed the state constraints. It assumes the accuracy of the model converges to a certain level in a finite time and does not request the Lyapunov function always decrease for relaxing the stability constraints. Based on the idea proposed in [17], where a non-increasing set updated every time step is used to describe system parameters uncertainty, the research in [18] developed an adaptive method for nonlinear system accounting for parameters uncertainty and exogenous disturbances under min-max MPC framework and Set-Membership identification. The algorithm needs to online solve a non-convex max-min optimization problem which makes the nonlinear version of this algorithm very time-consuming. In the GP model-based, MPC proposed in Ref. [11], the estimation of square errors of the GP at the current state is used to update the Lyapunov constraints. The MPC theoretically guarantees the steady-state error of the closed-loop system continues to decrease with the increase of the model accuracy. It can be seen from above that the idea of online updating the constraints for the conservatism reducing according to the estimation of the time-varying boundaries of model mismatch has been popular in the design of MPC. However, the methods to get the information on model mismatch online, and to use this information to modify the control design for better performance for different machine-learning-based methods are still in development, especially for nonlinear systems.

Koopman operator, which aims at finding an approximator close to the nonlinear system, is firstly introduced in [19]. Ref [19, 20] represented a nonlinear system by the linear operator in the infinite dimension. It lifts the state space of the nonlinear system to a higher dimensional space where the dynamic of lifted states is linear. In actual engineering practice, since we can only compute the ODE in the finite dimension, the method of the Koopman operator will lead to an error if the lifted state space is not closed in finite dimensions [19–22]. Ref. [23] proposed the method of lifting the data snapshots into a suitable finite-dimensional function space and identification of the infinitesimal generator of the Koopman semigroup. Ref. [24] aimed at identifying the linear Koopman operator in the space of observables, and did not require the estimation of the state time derivatives. Inspired by the [11, 18, 25], considering the nested form of the Set-Membership (SM) identification

method [18, 26, 27] and the linear characteristic of the system model in the lifting space. This paper will use the Koopman operator integrating SM identification method to design the learning-based MPC where the Koopman approximation model is worked as a predictive model for decreasing the computational complexity and getting continuing improvement of the performance.

In this paper, we focus on the design of an MPC for a class of nonlinear systems with exogenous disturbances and time-varying dynamics. Specifically, the adaptive MPC is based on the Lyapunov technique. An online updating approximator of the nonlinear continuous system is provided based on the Koopman operator, which can obtain very high accuracy with the lifted space dimension increasing. The model mismatch described by the size of the feasible parameter set (FPS) of the linear model is estimated at each control period. The Lyapunov constraint, which is also updated online, is based on an estimated model mismatch and the states in the original state space, which is convenient to set the Lyapunov function comprehensively compared to that defined in the lifted space. We proved that the designed MPC algorithm guarantees that the states will converge to a small region near the equilibrium point. Moreover, with the increasing accuracy of the Koopman model, the region that the states converge to will be minimized. This method could reduce the computational complexity and make it comparable to that of MPC which used a linear dynamical system. Simulation results show that the performance of the closed-loop system is improved.

The remainder is organized as follows. In Section 2, the problem setup is introduced. In Section 3, the system identification and the identification error which will be applied in the stability constraints are presented. In Section 4, the Adaptive Lyapunov-based MPC based on a shrinking uncertainty set is proposed. In Section 5, the stability analysis of the proposed ALMPC is carried out. A numerical example is presented in Section 6. In Section 7, conclusions are provided.

# 2 Preliminary

## 2.1 Notation

The operator $|\cdot|$ is used to represent the Euclidean norm of a vector. The transpose of a vector $x$ is denoted by $x^{\mathrm{T}}$. A Lyapunov level set $\Omega_\rho$ represents the set $\Omega_\rho := \{x \in \mathbb{R}^{n_x} | 0 \leq V(x) \leq \rho\}$, where $V(x) : \mathbb{R}^{n_x} \to R_{\geq 0}$ is a scalar function. Operator '/' indicates set subtraction, which is $\Omega_\rho / \Omega_{\rho_s} = \{x \in \mathbb{R}^{n_x} | x \in \Omega_\rho, x \notin \Omega_{\rho_s}\}$. A continuous function $\alpha : [0, a) \to [0, \infty)$ is called class $\mathcal{K}$ function if it is strictly increasing and satisfies $\alpha(0) = 0$.

## 2.2 Class of System

Consider a class of continuous nonlinear system

$$\dot{x} = f(x(t)) + g(x(t))u(t) + \omega(t) \tag{1}$$

where $x \in \mathbb{R}^{n_x}$ is the state of the nonlinear system; $u \in \mathbb{R}^{n_u}$ is the input variable; $\omega(t) \in \mathbb{W}$ is the disturbance vector; $f(x) : \mathbb{R}^{n_x+n_u} \to \mathbb{R}^{n_x}$ is sufficient smooth mappings. The origin $(x(t), u(t)) = (0, 0)$ is an equilibrium point of the unforced nominal system. The state constraint is defined by $x \in \mathcal{X} \subseteq \mathbb{R}^{n_x}(0 \in \mathcal{X})$ and the control input is restricted by $u \in \mathcal{U} := \{u \in \mathbb{R}^{n_u} : u \leq u_{max}\}$ where $u_{max}$ is the magnitude of the input constraint. The disturbance constraint is defined by $\omega \in \mathcal{W} := \{\omega \in \mathbb{R}^{n_x} : |\omega| \leq \delta, \delta > 0\}$.

In particular, we are looking for an approximator possessing an affine nonlinear structure that is suitable for general control design methodologies such as Sontag control. The predictors investigated are assumed to be in the form of a controlled dynamical system

$$\dot{x}(t) = f_m(x, \theta) + g_m(x, \theta)u(t) + \omega(t) + \omega_m(t) \tag{2}$$

where, $f(x)$ and $g(x)$ are both smooth mappings. $\theta$ is the parameter of the approximator and $\theta \in [\theta_L, \theta_H] \subset \mathcal{R}^{n_\theta}$. $\omega_m(t)$ is the error between the approximation and the real system. It includes two parts: $\omega_s$ and $\omega_e$. $\omega_s$ is the structural error and $\omega_e(t)$ is the error caused by inaccurate model parameters due to the inefficient data set used in model identification. The error $\omega_s(t)$ and $\omega_m(t)$ are both bounded, that is $|\omega_m(t)| \leq \delta_m$ and $|\omega_s| \leq \delta_s$.

In this paper, the approximator (2) of the dynamical system (1) will be derived within the Koopman operator framework.

## 2.3 Control Lyapunov Function

There exists a stabilizing control law $u = h(x)$, $u \in \mathcal{U}$, which will render the closed-loop nominal system asymptotically stable in the sense that there exists a continuously differentiable Control Lyapunov function $V(x)$ while states and control action satisfy constraints respectively for system (2). According to the Reverse Lyapunov Theorem, the assumption above implies that there exist constants $\alpha_i (i = 1, 2, \cdots, 4)$, for $\forall \theta \in [\theta_L, \theta_H]$, that render the nominal closed-loop system of (2), satisfy the following inequalities:

$$\alpha_1 |x|^2 \leq V(x) \leq \alpha_2 |x|^2 \tag{3a}$$

$$\frac{\partial V(x)}{\partial x} [f_m(x(t), \theta) + g_m(x(t), \theta)h(x, \theta)] \leq -\alpha_3 |x|^2 \tag{3b}$$

$$\left|\frac{\partial V(x)}{\partial x}\right| \leq \alpha_4 |x| \tag{3c}$$

where $V(x)$ is continuously differentiable.

# 3 Approximation with Koopman Operator and Set-Membership Method

## 3.1 Koopman Approximation

Consider a continuous-time dynamical system, given by:

$$\dot{x} = f(x) \tag{4}$$

where $x \in M$ is an n-dimensional state on a smooth manifold M. The vector field f is an element of the tangent bundle $T\ M$ of $M$, such that $f(x) \in T_x M$. Note that in many cases we dispense with manifolds and choose $M \subset \mathbb{R}^n$ and $f$ a Lipschitz continuous function. For a given time $t$, we may consider the flow map $F_t : M \to M$, which maps the state $z(t_0)$ forward time $t$ into the future to $z(t_0 + t)$, according to:

$$\mathbf{F}_t\left(\mathbf{x}\left(t_0\right)\right) = \mathbf{x}\left(t_0 + t\right) = \mathbf{x}\left(t_0\right) + \int_{t_0}^{t_0+t} \mathbf{f}(\mathbf{x}(\tau))d\tau \tag{5}$$

The Koopman operator $\mathcal{K}_t$ is an infinite-dimensional linear operator that acts on observable functions $\varphi$ as:

$$\mathcal{K}_t\varphi = \varphi \circ \mathbf{F}_t \tag{6}$$

where $\circ$ is the composition operator, so that:

$$\mathcal{K}_t\varphi\left(\mathbf{x}_k\right) = \varphi\left(\mathbf{F}_t\left(\mathbf{x}_k\right)\right) = \varphi\left(\mathbf{x}_{k+1}\right) \tag{7}$$

In other words, the Koopman operator $\mathcal{K}_t$ defines an infinite-dimensional nonlinear dynamical system that advances the observation of the state $\varphi(x_k)$ to the next time step. Note that this is true for any observable function $\varphi$ and any point $x_k \in M$. We may also describe the continuous-time version of the Koopman dynamical system in Eq (6) with the infinitesimal generator $\mathcal{K}$ of the one-parameter family of transformations $\mathcal{K}_t$ [45]:

$$\frac{d}{dt}\varphi(x) = \mathcal{K}\varphi = \lim_{t\to 0}\frac{\mathcal{K}_t\varphi - \varphi}{t} = \frac{\partial\varphi(x)}{\partial x}\dot{x} = \nabla\varphi(x)f(x) \tag{8}$$

The linear dynamical systems in Eqs (7) and (6) are analogous to the dynamical systems in Eqs (1) and (3), respectively. It is important to note that the original state $x$ may be observable, and the infinite-dimensional operator $\mathcal{K}_t$ will advance this observable function. Again, for Hamiltonian systems, the infinitesimal generator $\mathcal{K}$ is self-adjoint.

To transfer the model into an affine linear system, we select the lifting function in the following form.

$$\Phi(x,u) = \left[\ \varphi^{\mathrm{T}}, (\psi u)^{\mathrm{T}}\ \right]^{T} \tag{9a}$$

$$= \left[\ \varphi^{\mathrm{T}}(x), \varphi^{\mathrm{T}}(x)u_1, \varphi^{\mathrm{T}}(x)u_2, \cdots, \varphi^{\mathrm{T}}(x)u_m\ \right]^{\mathrm{T}} \tag{9b}$$

$$\varphi = \left[\ \varphi_1(x), \varphi_2(x), \cdots, \varphi_{n_K}(x)\ \right]^{\mathrm{T}} \tag{9c}$$

$$\psi = \mathrm{diag}_m\{\varphi(x)\} \tag{9d}$$

According to the definition of the Koopman operator, the system (9a) can be represented as a system with the linear operator in a lifting space

$$\dot{\Phi}(x,u) = \mathcal{K}\Phi(x,u) + \omega_m \tag{10}$$

where $\Phi(x,u) \in \mathcal{F}^{n_k(n_u+1)\times 1}$ is the lifting vector function which contains the primer modes of system (10) are selected, the $\omega_m$ is the mismatch caused by the ignored modes. When the lifting function $\varphi$ is an infinite dimension radius function or it makes the lifting space close $\omega_m = 0$.

Further select the first $n_x$ state of $x$ that is $\varphi_i = x_i$, $i = 1, 2, \ldots, n_x$. then it has

$$\dot{x}(t) = \theta_f\varphi(x(t)) + \theta_g\psi(x(t))u(t) + \omega_m \tag{11a}$$

$$= \theta_f\varphi(x(t)) + \sum_{i=1}^{m}\theta_{g_i}\varphi(x(t))u_i(t) + \omega_m \tag{11b}$$

where $\theta_f = \mathcal{K}_{\{1:n_x, 1:n_K\}}$, $\theta_g = \mathcal{K}_{\{1:n_x, n_K+1:n_K(n_u-1)\}}$. $\theta_{g_i}$ is the $i^{th}$ column vector of $\theta_g$.

System (11a) is an affine nonlinear system, and which is linear in parameter.

*Remark* 3.1. When the lifting space is not close, generally the dimension of the lifting space is infinite. In this case, we can select a finite dimension which is the major mode of system in the lifting space. The $\omega_m$ express the errors caused by the ignoring modes. In (11a) The selection of $\varphi$ can be any function, a simple way is to select $\varphi = [x \quad x^2 \quad \ldots \quad x^n]$. In this way, the $f_m(x)$ and $g_m(x)$ becomes a polynomial approximation of $f(x)$ and $g(x)$.

## 3.2 Control Lyapunov Function in Original State Space

There exists a stabilizing control law $u = h(x)$ which will render the closed-loop nominal system asymptotically stable in the sense that there exists a continuously differentiable Control Lyapunov function $V(x)$ while states and control action satisfy constraints respectively for system (11a). According to the Reverse Lyapunov Theorem, the assumption above implies that there exist constants $\alpha_i (i = 1, 2, \cdots, 4)$ that render the nominal closed-loop system of (11a) satisfy the following inequalities:

$$\alpha_1 |x|^2 \leq V(x) \leq \alpha_2 |x|^2 \tag{12a}$$

$$\frac{\partial V(x)}{\partial x}[\theta_f \varphi(x(t)) + \theta_g \psi(x(t))u(t)] \leq -\alpha_3 |x|^2 \tag{12b}$$

$$\left|\frac{\partial V(x)}{\partial x}\right| \leq \alpha_4 |x| \tag{12c}$$

where $V(x)$ is continuously differentiable.

The stabilizing control law $h(x)$ can be chosen as the Sontag control law in [28]

$$\begin{aligned} b(x) &= \begin{cases} -\frac{L_{\tilde{f}}V + \sqrt{L_{\tilde{f}}V^2 + \lambda L_{\tilde{g}}V^4}}{L_{\tilde{g}}V}, & \text{if } L_{\tilde{g}}V \neq 0 \\ 0, & \text{if } L_{\tilde{g}}V = 0 \end{cases} \\ h(x) &= \begin{cases} u_{min}, & \text{if } b(x) < u_{min} \\ b(x), & \text{if } u_{min} \leq b(x) \leq u_{max} \\ u_{max}, & \text{if } b(x) > u_{max} \end{cases} \end{aligned} \tag{13}$$

where $L_{\tilde{f}}V = \frac{\partial V(x)}{\partial x}\theta_f \varphi(x(t))$, $L_{\tilde{g}}V = \frac{\partial V(x)}{\partial x}\theta_g \psi(x(t))$ and $\lambda$ is a positive number satisfying $\lambda \in (0, 1)$. The stabilizing control law $u = h(x)$ which will render the closed-loop nominal system asymptotically stable in the sense that there exists a continuously differentiable Control Lyapunov function $V(x)$ while states and control actions satisfy constraints respectively for the system.

Based on (12), a region $\phi_u$ where the time-derivative of $V(x)$ is rendered negative under the control action $u = Kx$. Then the closed-loop stability region $\Omega_\rho$ for system (1) is given by $\Omega_\rho = \{x \in \mathbb{R}^{n_x} | V(x) < \rho\}$, where $\rho$ is chosen such that $\Omega_\rho \subseteq \phi_u$.

It should be noticed that for $u = Kx$ can steer the state of the actual nonlinear system into a small region, $\Omega_{\rho_{min}}$ depends on the value of $\delta_m$. In the inside of region $\Omega_{\rho_{min}}$, (12) can not be satisfied.

The modeled system satisfy the following Lipschitz condition for all $x, x' \in \Omega_\rho$, $u \in \mathcal{U}$.

$$|\theta_f \varphi(x) + \theta_g \psi(x)u(t)| \leq M \tag{14}$$

where $M$ is a constant.

Then, $\forall \theta, \theta' \in \Theta, x, x' \in \mathcal{X}$, we can get

$$\begin{aligned} &|\frac{\partial V(x')}{\partial x'}(\theta'_f \varphi(x') + \theta'_g \psi(x')u(t) + \omega(t) + \omega_m(t)) - \frac{\partial V(x)}{\partial x}(\theta_f \varphi(x) + \theta_g \psi(x)u(t))| \\ \leq &L_x |x' - x| + L_\theta |\theta' - \theta| + L_\omega |\omega| + L_{\omega_m} |\omega_m| \end{aligned} \tag{15}$$

where $L_x$ and $L_\theta$, $L_\omega$ and $L_{\omega_m}$are the maximum Lipschitz constants for $\forall x', x \in \mathcal{X}$, $\theta, \theta' \in \Theta$.

### 3.3 Set-Membership Parameter Identification

Set-Membership identification is a method for constructing a mathematical model of a dynamic system from experimental data [26, 27, 29, 30], which provides a set of all possible plant models that are consistent with the exogenous disturbance boundary and the measured data.

In lots of system identification literature, researchers generally assume that the system noise is Stochastic Process and satisfies certain assumptions. But it is difficult for the actual system to verify this assumption, which leads to two main contradictions: first, because actual systems are quite complex, simple mathematical models can not always be used as their system models; second, since the model type and noise are artificially assumed, it seems that all systems can obtain a model that is arbitrarily close to the real system through identification. These contradictions promote the research of Set-Membership Identification [27, 29].

The biggest feature of Set-Membership Identification is that the prior distribution of the noise is not necessary to be acquired and it only needs the upper and lower bounds of the noise. According to the input and output data of the system, a set (Feasible Parameter Set, FPS) including the real parameters can be obtained; Since it could provide an explicit description of the possible model set, it is very suitable for incorporating online updating robust considerations into MPC design.

In this paper, online identification through Set-Membership is used to update the parameters of the linear model as which the nonlinear system is described by the Koopman operator. The identification algorithm is proposed in [29] and is extended to MIMO later. Online identification can not only update the linear model using continuously emerging data but also provide a feasible set of linear model parameters which can benefit robust controller design. Since FPS is usually irregular, researchers usually use regular geometric sets to approximate FPS, such as ellipsoids, cuboids, and polygons. In this paper, a hyper-dimensional ellipsoid is used to approximate FPS.

At time instant $t_k$, if the current system state $x(t_k)$ is known, the parameters and the feasible parameter set of the model are updated. To express simply, rewrite the system model as

$$\dot{x}(t_k) = \theta_o^{\mathrm{T}} x(t_k) + \bar{\omega}(t_k) \tag{16}$$

where $x(t_k)^{\mathrm{T}} = [\mathbf{\Phi}\left(x(t_k)\right)^{\mathrm{T}} \ \ \mathbf{\Phi}\left(x(t_k)\right) u(t_k)^{\mathrm{T}}]$, $\theta_o^{\mathrm{T}} = [A\ B]$, and $\bar{\omega}$ includes $\omega$ and $\omega_m$.

At $t_{k-1}$, the feasible parameter set can be approximated by an ellipsoid:

$$\Theta_{t_{k-1}} = \left\{\theta | tr((\theta - \theta_c(t_{k-1}))^{\mathrm{T}} P_{t_{k-1}}^{-1} (\theta_i - \theta_c(t_{k-1}))) \leq \sigma_{t_{k-1}}^2\right\} \tag{17}$$

where $P_{t_{k-1}} \in \mathcal{R}^{(N+n_uN)(N+n_uN)}$ is the weight matrix; $\theta_c(t_{k-1})$ is the model parameter identified at time $t_{k-1}$; $\theta_{t_{k-1}}^2$ is a scalar and $tr(\cdot)$ represents the trace of matrix.

Assume that $S_{t_k}$ is the feasible parameter set decided by $\dot{x}(t_k)$ and the constrain of disturbance

$\bar{\omega} \in \mathbb{W} := \{\bar{\omega} \in R^{n_\omega} s.t. |\bar{\omega}| \leq \delta_{\bar{\omega}}, \delta_{\bar{\omega}} > 0\}$, which is

$$S_k = \left\{\theta \left| \left|\dot{x}(t_k) - \theta^{\mathrm{T}} x(t_k)\right|^2 < \delta_{\bar{\omega}}^2 \right.\right\} \tag{18}$$

Obviously, the feasible parameter set at $t_k$ is the intersection of $\Theta_{t_{k-1}}$ and $S_k$. Considering that this intersection is not necessarily still an ellipsoid, an ellipsoid $\Theta_{t_k}$ which satisfies $(\Theta_{t_{k-1}} \bigcap S_k) \subset \Theta_{t_k}$ is adopted to approximate this intersection, then $\Theta_{t_k}$ can be written as

$$\Theta_{t_k} = \left\{\theta \mid tr((\theta - \theta_c(t_{k-1}))^{\mathrm{T}} P_{t_{k-1}} (\theta - \theta_c(t_{k-1}))) + \left|\dot{x}(t_k) - \theta^{\mathrm{T}} x(t_k)\right|^2 \leq \sigma_{t_k}^2 + \delta_{\bar{\omega}}^2 \right\} \tag{19}$$

rearrange the above equation, we can get

$$\Theta_{t_k} = \left\{\theta | tr((\theta - \theta_c(t_k))^{\mathrm{T}} P_{t_k}^{-1} (\theta - \theta_c(t_k))) \leq 1\right\} \tag{20}$$

where

$$\theta_c(t_k) = \theta_c(t_{k-1}) + a_{t_k} P_{t_{k-1}} x(t_k) \left[\dot{x}(t_k)^{\mathrm{T}} - x(t_k)^{\mathrm{T}} \theta_c(t_{k-1})\right] \tag{21a}$$

$$P_{t_k} = b_{t_k} (P_{t_{k-1}} - a_{t_k} P_{t_{k-1}} x(t_k) x(t_k)^{\mathrm{T}} P_{t_{k-1}}) \tag{21b}$$

$$a_{t_k} = 1/(1 + x(t_k)^{\mathrm{T}} P_{t_{k-1}} x(t_k)) \tag{21c}$$

$$b_k = 1 + \delta_{t_k} - a_{t_k} tr\left\{\left[\dot{x}(t_k) - \theta_c^{\mathrm{T}}(t_{k-1}) x(t_k)\right] \left[\dot{x}(t_k)^{\mathrm{T}} - x(t_k)^{\mathrm{T}} \theta_c(t_{k-1})\right]\right\} \tag{21d}$$

*Remark* 3.2. The outer bound of the intersection $\Theta_{i,t_{k-1}} \bigcap S_{i,k}$ is approximated by an ellipsoid, which is (19), and after organizing (19), we can get (20).

The $\theta_c(t_k)$ in the FPS is the identification result used in (2), that is $\theta_c^{\mathrm{T}}(t_k) = [A(t_k)\ B(t_k)]$.

# 4 Adaptive Lyapunov-based MPC

In this section, an Adaptive Lyapunov-based MPC (ALMPC) scheme is proposed. In the ALMPC, a linear model described by the Koopman operator is used as the predictive model for optimization. Set-Membership identification in the previous section is used to update the parameters of the linear model. The updating of the parameters will also change the stability constraints and make the unstable region narrow.

The proposed ALMPC scheme provides a permissible convergence region such that the closed-loop system with any initial state $x_0$ within the predefined region will eventually converge to a small neighborhood of the origin.

## 4.1 ALMPC Design

This section shows the details of the ALMPC design. At each sampling time $t_k$, the parameters in (11a) will be updated through the Set-Membership identification in the previous section. Based on the updated model, the ALMPC is designed through the following optimization problem:

$$\min_{u\in S(\Delta)} \int_{t_k}^{t_{k+N}} l(\tilde{x}(\tau), u(\tau))d(\tau) \tag{22a}$$

$$\text{s.t.} \quad \dot{\tilde{x}} = \theta_f \varphi(\tilde{x}(t)) + \theta_g \psi(\tilde{x}(t))u(t) \tag{22b}$$

$$u(t) \in \mathcal{U}, t \in [t_k, t_{k+N}] \tag{22c}$$

$$\tilde{x}(t_k) = x(t_k) \tag{22d}$$

$$\begin{aligned} &\frac{\partial V(x(t_k))}{\partial x}\theta_f(t_k)\varphi(x(t_k)) + \theta_g(t_k)\psi(x(t_k))u(t_k) \\ &\quad \leq \frac{\partial V(x(t_k))}{\partial x}\left(\theta_f(t_k)\varphi(x(t_k)) + \theta_g(t_k)\psi(x(t_k))h(x(t_k), \theta_{t_k})\right), \quad \text{if } x(t_k) \in \Omega_\rho / \Omega_{\rho_{min}}(t_k) \end{aligned} \tag{22e}$$

$$V(x(t)) < \rho_s(t_k), \quad \text{if } x(t_k) \in \Omega_{\rho_s}(t_k), t \in [t_k, t_{k+N}] \tag{22f}$$

In the ALMPC optimal problem of (22), the constraint (22b) is the predictive model which is described as a linear model by the Koopman operator. The constraint (22c) is the constraint of the input. The constraint (22d) defines the states at time $t_k$. The constraint (22e) can guarantee the rate of convergence of the Lyapunov function under the input $u(t)$ is faster than the Sontag control law $h(x(t_k), \theta_{t_k}))$. The stability of the system can be ensured by the constraint (22f). The continuous problem can be programmed by sampling. $\Delta$ is the sampling time. Thus $u(\tau) = u(t_{k+i}), \tau \in [t_{k+i}, t_{k+i+1})$, $i = 0, 1, \ldots, N-1$, and $N$ is the prediction horizon. By solving the optimization problem of (22), an optimal trajectory of the manipulated input, $u^*(0|t_k), \cdots, u^*(N-1|t_k)$ is obtained.

At each time $t_k$, the proposed method updates the parameters in (21) firstly. The second step is to update the constraints which are corresponding to the parameters. Finally, the optimization problem (22) will be solved and $u^*(t_k)$ is obtained. During the period from $t_k$ to $t_{k+1}$, the control action $u(\tau) = u^*(t_k)$ is implemented on the actual system.

*Remark* 4.1. It can be seen from (10) which is a linear model, $x$ is one of the elements of the state vector $\Phi(x)$. $\Phi(x(t))$ can be calculated as the form of $\Phi(x(t)) = M\Phi(x(t_0)) + \int_{t_0}^{t} Nu(\tau)d\tau$, where $M$ and $N$ are matrixes and only related to time $t$. Considering the input $u$ is piece-wise, $\Phi(x(t))$ can be written as the linear combination of $u(t_k), u(t_{k+1}), \ldots$, so $x$ is also an affine of the input $u(t)$. In other words, (22b) is an affine of $u$ and convex. Since $\theta_f$, $\theta_g$, $\varphi(x)$, $\psi(x)$, $h(x, \theta)$ and the partial of $V(x)$ can be acquired by the state $x$ and the parameters obtained by online identification, the inequality

of (22e) is linear inequality of $u(t)$ and is convex. As we choose the Lyapunov function $V(x)$ as a quadratic form, (22f) is a quadratic constraint. The problem is quadratic. So the optimazation problem is QCQP. These make solving the ALMPC optimization problem not time-consuming.

In this paper, we assume there is an unstable region $\Omega_{\rho_s}$, and through the decreasing online identification error bound and robust control law, the unstable region $\Omega_{\rho_s}$ can be minimized. Here, we provide the updating of unstable region size $\rho_s$ as follows.

$$\rho_s(t_k) = \left(L_x M\Delta + L_\theta \delta_\theta + L_{\omega_s}\delta_s + L_\omega \delta\right)\frac{\alpha_2}{\alpha_3} + \delta_{\rho_s} \tag{23}$$

where $\delta_\theta = \lambda_{\max}^{\frac{1}{2}}(P_{t_k}^{\mathrm{T}} P_{t_k})$ are the Lipschitz constants.

*Remark* 4.2. Since there exists a stabilizing control law that could stabilize all the models in the original model set, with the increasing accuracy of the feasible model set, the original stabilizing region $\Omega_\rho$ is non-decreasing, which means that the feasibility of the optimization problem could be guaranteed. As the Set-Membership identification algorithm could provide decreasing identification variance, then the size of the unstable region $\rho_s$ could be rendered decreasing. Meanwhile, the stabilizing Sontag control law is updated using the identified system parameters. Based on the more and more accurate identification results, the conservatism caused by model mismatch could be reduced.

# 5 Analysis

## 5.1 Stability analysis

In this section, the stability properties of the proposed ALMPC of (22) for the nonlinear system, i.e. (2) are proved. To proceed, the following Proposition is proposed first.

*Proposition* 5.1. Consider the Lyapunov function $V(\cdot)$ of the system (1). There exists a quadratic function $F_V(\cdot)$ such that

$$V(x) \leq V(\bar{x}) + F_V(|x - \bar{x}|) \tag{24}$$

for all $x, \bar{x} \in \Omega_\rho$ with

$$F_V(s) = \alpha_4 \sqrt{\frac{\rho}{\alpha_1}} + M_V s^2 \tag{25}$$

where $M_V$ is a positive constant.

*Theorem* 5.1. Consider the system (2) in closed-loop under the ALMPC of (22) with the online Set-Membership identification. Under the property of (15), with sampling time $\Delta > 0$, $\rho > \rho_s$ satisfying:

$$-\alpha_3 \frac{\rho_s}{\alpha_2} + L_x M \Delta + L_\omega \delta + L_{\omega_m} \delta_m + L_\theta \delta_\theta(t_\infty) < 0 \tag{26}$$

if $x(t_0) \in \Omega_\rho$ and $\rho_{min} \leq \rho$ where

$$\rho_{min} = \rho_s + F_V(M\Delta) \tag{27}$$

then the state of the closed-loop system is ultimately bounded in $\Omega_{\rho_{min}}$.

*Proof.* When $x(t_k) \in \Omega_\rho / \Omega_{\rho_s}$, from (22e) and Lyapunov condition of $\dot{V}$, i.e. $\frac{\partial V(x(t_k))}{\partial x}(\theta_f(t_k)\varphi(x(t_k)) + \theta_g(t_k)\psi(x(t_k))h(x(t_k), \theta_{t_k})) \leq -\alpha_3(t_k)\left|x\right|^2$, the following inequality is obtained:

$$\begin{aligned} &\frac{\partial V(x(t_k))}{\partial x}(\theta_f(t_k)\varphi(x(t_k)) + \theta_g(t_k)\psi(x(t_k))u(t_k)) \\ \leq &\frac{\partial V(x(t_k))}{\partial x}(\theta_f(t_k)\varphi(x(t_k)) + \theta_g(t_k)\psi(x(t_k))h(x(t_k), \theta_{t_k})) \\ \leq &-\alpha_3(t_k)\left|x(t_k)\right|^2 \end{aligned} \tag{28}$$

$\forall \tau \in [t_k, t_{k+1})$, the time derivative of the Lyapunov function of system (2), with the implements of the optimal piece-wise constant control input $u(\tau) = u^*(t_k)$, is given by:

$$\dot{V}(x(\tau)) = \frac{\partial V(x(\tau))}{\partial x}(\theta_f(\tau)\varphi(x(\tau)) + \theta_g(\tau)\psi(x(\tau))u^*(t_k) + \omega(\tau) + \omega_m(\tau)) \tag{29}$$

Combing (28) and (29), we have:

$$\begin{aligned} \dot{V}(x(\tau)) \leq &-\alpha_3(t_k)\left|x(t_k)\right|^2 \\ &+ \frac{\partial V(x(\tau))}{\partial x}(\theta_f(\tau)\varphi(x(\tau)) + \theta_g(\tau)\psi(x(\tau))u^*(t_k) + \omega(\tau) + \omega_m(\tau) \\ &- \frac{\partial V(x(t_k))}{\partial x}(\theta_f(t_k)\varphi(x(t_k)) + \theta_g(t_k)\psi(x(t_k))u(t_k)) \end{aligned} \tag{30}$$

Based on the Lipschitz condition of $\dot{V}$, i.e. (15), the above inequality can be written as follows:

$$\begin{aligned}\dot{V}(x(\tau)) \leq & -\alpha_3(t_k)\left|x(t_k)\right|^2 + L_x\left|x-\bar{x}\right| + L_\omega\left|\omega(\tau)\right| + L_{\omega_m}\left|\omega_m(\tau)\right| + L_\theta\left|\bar{\delta}_\theta(\tau)\right| \\ = & -\alpha_3(t_k)\left|x(t_k)\right|^2 + L_x\left|x-\bar{x}\right| + L_\omega\delta + L_{\omega_m}\delta_m(t_k) + L_\theta\delta_\theta(t_k)\end{aligned} \tag{31}$$

Considering the property of the linear system, i.e. (14), we can obtain:

$$|x(\tau) - x(t_k)| \leq M\Delta \tag{32}$$

Since $x(t_k) \in \Omega_\rho/\Omega_{\rho_s}$, taking (12a) into account, it has:

$$|x(t_k)| \geq \sqrt{\frac{\rho_s}{\alpha_2}} \tag{33}$$

Thus, (31) can be rewritten as :

$$\dot{V}(x(\tau)) \leq -\alpha_3(t_k)\frac{\rho_s}{\alpha_2} + L_x M\Delta + L_\omega\delta + L_{\omega_m}\delta_m(t_k) + L_\theta\delta_\theta(t_k) < 0 \tag{34}$$

Integrating the above inequality from $t_k$ to $t_{k+1}$, we have:

$$V(x(t_{k+1})) < V(x(t_k)) \tag{35}$$

If $x(t_k)$ is in $\Omega_{\rho_s}$, with *Proposition 5.1* and the property of linear system (14), we obtain

$$\begin{aligned}V(x(t_{k+1})) \leq & V(x(t_k)) + F_V(|x(t_{k+1} - x(t_k))|) \\ \leq & \rho_s + F_V(M\Delta) = \rho_{min}\end{aligned} \tag{36}$$

When $t \to \infty$, we first choose $\alpha_3$ which satisfies the (34). $\rho_s(t_k)$ will decrease and the state will converge to the set point. If the $\delta_\theta$ can not decrease, we can get the minimal $\rho_s$ and $\rho_s = \rho_s(\infty) < \rho_s(t_0)$. $\rho_s$ satisfies (26) and the state of the system will enter the region of $\Omega_{\rho_s}$. Once the state enters the region, it will maintain in the region of $\Omega_{\rho_s}$. In other words, the state will finally converge to the region of $\Omega_{\rho_s}$ and be stable in the region of $\Omega_{\rho_s}$.

In sum, if the state $x(t_k) \in \Omega_{rho}(t_k)/\Omega_{rho_s}(t_k)$, $V(x(t_{k+1})) < V(x(t_k))$ will be satisfied. If the state $x(t) \in \Omega_{\rho_s}(t)$, $V(x(t_{k+1})) < \rho_{\min}$ is affirmed and using (35) and (36) recursively, the subsequent system states will ultimately bounded in the minimal $\Omega_{\rho_{min}}$.

□

This proves *Thorem 5.1.*

*Theorem* 5.2. If persistent excitation is implemented in the identification, the error $\delta_\theta$ will be a constant. (26) will be rewritten as:

$$-\alpha_3 \frac{\rho_s}{\alpha_2} + L_x M \Delta + L_\omega \delta + L_{\omega_m} \delta_m + L_\theta \delta_\theta < 0 \tag{37}$$

The region size of $\Omega_{\rho_s}$ is the minimum and will not change. According to Proof. (5.1), the $V(x)$ is decreasing and the state will finally enter the region of $\Omega_{\rho_s}$ and maintain in it.

# 6 Simulation

In this section, an experimental example was carried out to verify the effectiveness of the proposed method.

## 6.1 Fluid Catalytic Cracking Unit Simulink

In this section, the Fluid Catalytic Cracking Unit (FCCU), which is one of the most important processes in the petroleum industry, is taken as an experimental example to verify the effectiveness of the proposed method. The FCC reactions make the crude oil which is a low valuable and high molecular weight hydrocarbon transform into more valuable products with lower molecular weight, such as diesel, gasoline, and kerosene. Fig.1 shows the schematic overview of the FCC process. The FCC unit includes a riser, a stripper, and a regenerator. The main reactions take place in the riser. The catalyst meets the crude oil at the riser entrance and rises with the catalytic cracking reactions. Under the action of the catalyst, the vaporized heavy gas oil cracks into smaller molecules which are more valuable. Coke, one of the by-products, attaches to the catalyst and decreases its activity. To boost the availability of the catalyst and increase its activity, the spent catalyst is separated from the hydrocarbons in the stripper and sent to the regenerator to remove the coke. In the regenerator,

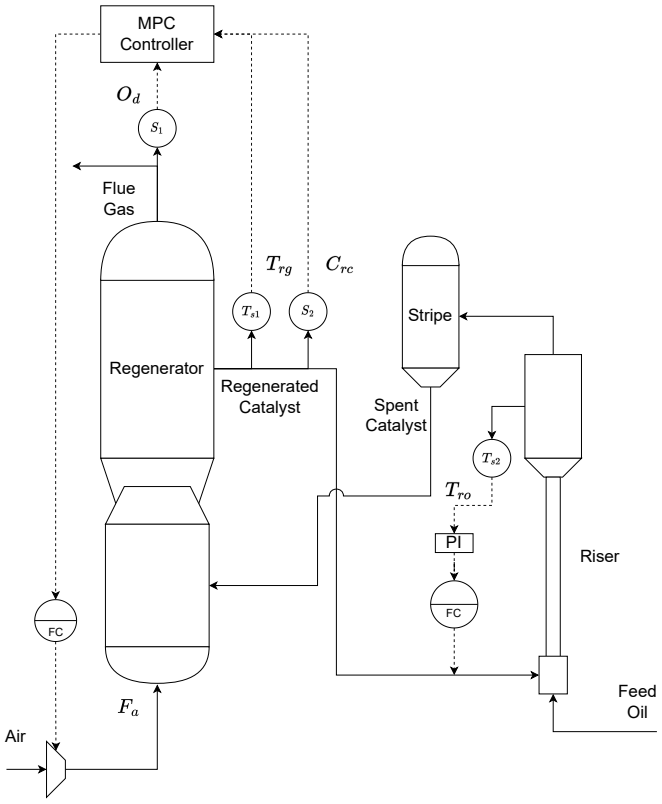


Figure 1: Schematic of the Fluid Catalytic Cracking unit

the coke which surrounds the spent catalyst's surface is burned with air. The catalyst is refreshed and circulated back to the inlet of the riser. This progress supplies the reaction heat of the riser.

The dynamics of the FCCU process can be described as follows:

### Riser Model and Stripper Model

The riser is modeled as a plug flow reactor. It is considered that the catalytic cracking reactions only occur in the riser. The catalytic cracking reactions in the riser obey the rules of mass balance and energy balance. According to the mass balance, the variations of the gas oil and gasoline are given as:

$$\frac{\mathrm{d}y_f}{\mathrm{d}z} = -K_1 y_f^2 \frac{F_{sc}}{F_{oil}} \Phi t_c \tag{38}$$

$$\frac{\mathrm{d}y_g}{\mathrm{d}z} = \left(\alpha_2 K_1 y_f^2 - K_3 y_g\right) \frac{F_{sc}}{F_{oil}} \Phi t_c \tag{39}$$

where

$$K_1\left(\Theta\right) = k_1 e^{\frac{-F_f}{RT_0(1+\Theta)}} \tag{40}$$

$$K_3\left(\Theta\right) = k_3 e^{\frac{-E_g}{RT_0(1+\Theta)}} \tag{41}$$

$$\Theta = (T(z) - T_0)/T_0 \tag{42}$$

$$\Phi = \phi_0 e^{-\alpha t_c \frac{F_{sc}}{F_{oil}} z} \tag{43}$$

$$\phi_0 = 1 - mC_{rc} \tag{44}$$

The $K_1 y_f^2 \frac{F_{sc}}{F_{oil}}$ and $K_3 y_g \frac{F_{sc}}{F_{oil}}$ represent the kinetics for the cracking of gas oil and gasoline respectively. $\Phi$ represents the deactivation of the catalyst caused by the coke deposition, of which $\phi_0$ represents the reduction in catalyst activity caused by the coke remaining on the catalyst after regeneration. $t_c$ is the residence time in the riser, and $\alpha = k_2/k_1$ is the fraction of the cracked gas oil which cracks to gasoline. $z$ is the height of the riser. The following equation is used to estimate the mass fraction of the produced coke:

$$C_{cat} = k_c \sqrt{\frac{t_c}{C_{rc}^N} e^{\frac{-E_{cf}}{RT_{ro}}}} \tag{45}$$

Thus, we can get the mass fraction of the coke on the catalyst leaving the riser by the following equation:

$$C_{sc} = C_{rc} + C_{cat} \tag{46}$$

Based on the energy balance, it has

$$\frac{\mathrm{d}\Theta}{\mathrm{d}z} = \frac{\Delta H_f F_f}{T_0 (F_s c_{ps} + F_f c_{po} + \lambda F_f c_{pd})} \frac{\mathrm{d}y_f}{\mathrm{d}z} \tag{47}$$

The stripper model is modified on the work of [31]. Note that there exists a common assumption that there are no reactions in the stripper. Assuming the stripping is effective, the only effect of the stripper will be to introduce a lag between the riser outlet and the catalyst return to the regenerator. This lag is modeled using an ideal mixing tank. According to the balances of mass and energy, the variations of the concentration of coke and the stripper's temperature can be calculated by following equations:

$$\frac{\mathrm{d}C_{st}}{\mathrm{d}t} = \frac{C_{sc} - C_{st}}{W_{st}} \tag{48}$$

$$\frac{\mathrm{d}T_{st}}{\mathrm{d}t} = \frac{F_{sc}}{W_{st} c_{pc}} (T_{ro} - T_{st}) \tag{49}$$

**Regenerator Model**

The regenerator model concludes the balance equations for coke, oxygen, and energy. Furthermore, we assume that the regenerator is working under the complete combustion mode. It means that the coke on the refresh catalyst is sufficiently small and can be neglected. The mass balances for the coke on the catalyst and oxygen are given as:

$$W \frac{\mathrm{d}C_{rc}}{\mathrm{d}t} = F_{sc} (C_{sc} - C_{rc}) - R_{cb} \tag{50}$$

$$W_a \frac{\mathrm{d}O_d}{\mathrm{d}t} = \frac{F_a}{M_a}(O_{in} - O_d) - \frac{1+1.5\theta}{(1+\theta)M_c} R_{cb} \tag{51}$$

$$\tag{52}$$

According to the energy balance, the variation of the temperature is given as:

$$\begin{aligned} W c_{pc} \frac{\mathrm{d}T_{rg}}{\mathrm{d}t} =& T_{st} F_{sc} c_{pc} + T_a F_a c_{pa} - T_{rg}(F_{sc} c_{pc} + F_a c_{pa}) \\ & - \left( \Delta H_{CO} + \frac{\theta}{1+\theta} \Delta H_{CO2} \right) \frac{R_{cb}}{M_c} \end{aligned} \tag{53}$$

where

$$R_{cb} = k_{cb} e^{\frac{-E_{cb}}{RT_{rg}}} O_d C_{rc} W \tag{54}$$

$$\theta = 1.1 + 0.0061(T_{rg} - 873) \tag{55}$$

$$\tag{56}$$

## 6.2 Simulation setting

Fig.2 shows how the simulation performs. Two computers are involved. Computer 1 accesses the input $u$, finishes the FCC process simulation, and calculates the state $x$. According to state $x$, Computer 2 solves the Koopman approximator based adaptive LMPC to get the input $u$. The network is implemented to let the computers exchange messages.

In this simulation, there exists a low-level PI control that makes the temperature of the riser's outlet reach a steady state in several seconds. Therefore, what we are concerned about is the regenerator. The temperature of the regenerator is related to the reaction speed and the combustion, the concentration of the oxygen can affect whether the coke can be burnt better or not, and the mass fraction of the coke has an influence on the activity of the refreshed catalyst. In view of above–mentioned reasons, we choose them as the states and the flow rate of the air as the input. In particular, the riser can reach the steady state in several seconds, but the regenerator needs dozens of minutes to reach the steady state. Thus, the model of the riser is considered a steady-state model and used for calculating the parameters in the regenerator model. The states and manipulative input of the regenerator are as follows:

$$x = \begin{bmatrix} C_{rc} & O_d & T_{rg} \end{bmatrix}^{\mathrm{T}} \qquad u = F_a \tag{57}$$

One simulation with Set-Membership Identification to update the model was done and another simulation without model update was designed to be a comparison.

Desired set points in FCC unit are chosen as $x_{sp} = [2.907 \times 10^{-3}, 4.286 \times 10^{-3}, 994.694]^T$ and $u_{sp} = 27.23$. The states constraints are given as $C_{rc} \in [1 \times 10^{-3}, 3.5 \times 10^{-3}]$, $O_d \in [3 \times 10^{-3}, 1.4 \times 10^{-2}]$ and $T_{rg} \in [980, 1000]\,\mathrm{K}$. The constraint of input $F_a$ is given by $F_a \in [23, 29.23]\,\mathrm{kg/s}$. The sampling

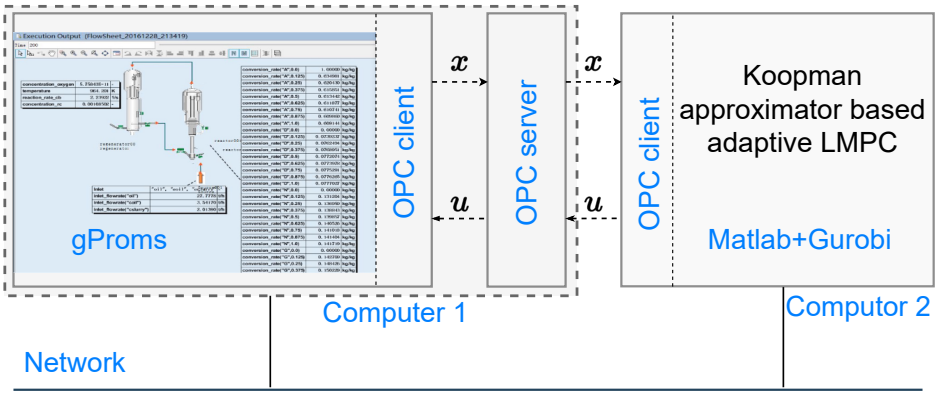


Figure 2: Simulation Structure

interval $\Delta = 0.001$h and integration interval $h_c = 0.0001$h. The prediction horizon $N$ is 10. The disturbance in this simulation is the fluctuation of the rate of coke combustion $R_{cb}$ in the regenerator, and it satisfies $|\omega| < 6.8788 \times 10^{-3}$. In the simulation, we chose the Lyapunov function $V(x)$ as the objective function. The matrix $P$ of $V(x)$ is $P = diag[1 \times 10^8, 1 \times 10^6, 1.1]$. More details of the parameters are shown in Table.1.

The simulation starts at $t_0 = 0h$ and stops at $t_f = 1h$ using Matlab in an AMD Radeon R7 with a frequency of 1.8GHz.

$$\Delta H_{CO} = -361465.3 + 16.23T_{rg} - 31.92 \times 10^{-4}T_{rg}^2 + 18.67 \times 10^{-7}T_{rg}^3 + \frac{1275299.0}{T_{rg}} \tag{58}$$

$$\Delta H_{CO2} = -284375 - 1.653T_{rg} + 29.51 \times 10^{-4}T_{rg}^2 + \frac{425588.2}{T_{rg}} \tag{59}$$

Table 1: parameters of the FCCU unit model

| **Notation** | **Description** | **Value** |
|---|---|---|
| $F_f$ | Feed Oil Flow Rate | $40.63kg/s$ |
| $T_f$ | Feed Oil Temperature | $400K$ |
| $E_f$ | Activation Energy For The Cracking of Gas Oil | $1.015\times10^5 J/mol$ |
| $E_g$ | Activation Energy For The Cracking of Gasoline | $1.126\times10^5 J/mol$ |
| $k_1$ | Reaction Rate Constant For The Total Rate of Cracking of Gas Oil | $9.6 \times 10^5 s^{-1}$ |
| $k_2$ | Reaction Rate Constant For The Rate of Cracking of Gas Oil To Gasoline | $7.2 \times 10^5 s^{-1}$ |
| $k_3$ | Reaction Rate Constant For The Rate of Cracking of Gasoline To Light Gases/Carbon | $4.22 \times 10^5 s^{-1}$ |
| $k_c$ | Reaction Rate Constant For The Production of Coke | $1.897 \times 10^{-2} s^{-1}$ |

Continued on next page

Table 1: parameters of the FCCU unit model (Continued)

| | | |
|---|---|---|
| $k_{cb}$ | Reaction Rate Constant For Coke Combustion Assuming Uniformly Distributed Oxygen In The Regenerator | $1.9 \times 10^8 s^{-1}$ |
| $R$ | Universal Gas Constant | 8.314 |
| $t_c$ | Residence Time In Riser | $9.6s$ |
| $m$ | Factor For The Dependence of The Initial Catalyst Activity On $C_{rc}$ | 80 |
| $\alpha_2$ | Fraction of The Gas Oil That Cracks Which Cracks To Gasoline | 0.75 |
| $\Delta H_f$ | Heat of Cracking | $506.2kJ/kg$ |
| $\Delta H_{CO}, \Delta H_{CO2}$ | Heat of Producing $CO, CO_2$ respectively | (58),(59) |
| $\lambda$ | Mass Flow Rate of Dispersion Steam/Mass Flow Rate of Feed Oil | 0.035 |
| $c_{pc}$ | Heat Capacity of Catalyst | $1.005kJ/kgK$ |
| $c_{po}$ | Heat Capacity of Oil | $3.1335kJ/kgK$ |
| $c_{pd}$ | Heat Capacity of Steam | $1.9kJ/kgK$ |
| $c_{pa}$ | Heat Capacity of Air | $1.074kJ/kgK$ |
| $W$ | Holdup of Catalyst In Regenerator | $175738kg$ |
| $W_a$ | Holdup of Air In The Regenerator | $20kmol$ |
| $O_{in}$ | Concentration of Oxygen In Air To Regenerator | 0.2136 |
| $M_c$ | Bulk Molecular Weight of Coke | 14 |
| $M_a$ | Molecular Weight of Air | 28.8544 |
| $T_a$ | Temperature of Air To The Regenerator | $320K$ |
| $E_{cf}$ | Activation Energy For Coke Formation | $41790J/mol$ |
| $E_{cb}$ | Activation Energy For Coke Combustion Assuming Uniformly Distributed Oxygen In The Regenerator | $41790J/mol$ |
| $N$ | Exponent For The Dependence of $C_{cat}$ on $C_{rc}$ | 0.4 |
| $W_{st}$ | Holdup of Catalyst In Separator | $17500kg$ |

## 6.3 Simulation Results

As fig.3 shows, we learned that whether the model is updated or not updated, each control law can make the system reach a steady and desired state. Fig.3 illustrates that at the beginning, each line changed at almost the same rate. However, with the proceeding of the identification, the blue line converged faster than the red line. The transient time of the blue line is $0.3h$ and that of the red line is $0.5h$. It means that to achieve the same aim, the proposed method required fewer episodes than the MPC without model update. In addition, the proposed method leads to a better control performance than the MPC without model update. Fig 4 shows the trajectory of the optimized manipulated control input. At $t = 0.5h$, it enters the steady region.

Fig.5 plots that the Lyapunov function $V(x)$ of each line decreased and the blue line converged faster than the red line. The enclosed area of the Lyapunov function $V(x)$ and time $t$ reflects the applicability and effectiveness of the control law. The area of the blue line is 2.2180 and the area of the red line is 3.0067. The difference between the two areas is 0.7887. It shows that the proposed method not only performs better in the speed of the convergence but also is about 26% greater than the MPC without model update.

Fig.6 is related to the update of Lipschitz constant $\delta_\theta$. The value of $\delta_\theta$ is the ratio of the semi-major axis of the set of $\theta$ and the length of the final $\theta$. It reflects the size of the set of $\theta$. With more data exciting the model, the result of the online identification became more accurate. We can verify this by the value of $\delta_\theta$. In Fig.6, $\delta_\theta$ decreased and finally reached 0.143.

Fig.7 provides more details on the trajectory of the state. The red line shows that the state $x$ converged with time going on and the trajectory finally reached the small little neighbor region of the set point. This proves the stability of the proposed control method.

Table.2 shows that the consumed time of the proposed method that solves the optimization problem is $0.0578s$ and that of the MPC with the first-principles model is $0.3727s$. We can find that the efficiency of the proposed method is 644.81% better than the MPC with the first-principles model.

Table 2: Comparasion of the time

| Nominal model | Time/s |
|---|---|
| Linear model with Koopman operator | 0.0578 |
| First-principles model | 0.3727 |

# 7 Conclusion

In this research, a Koopman approximator model-based ALMPC is proposed for nonlinear systems with external disturbances and time-varying dynamics. The nonlinear model is remodeled as a linear model building on the Koopman approximation framework. We design the parameters' update law of the linear model according to the method of Set-Membership identification which makes parameters bounded in a continuing shrinking set. It is not necessary to know the prior distribution of disturbances, but the min and max bound are enough. At each time instant, with the FPS updating, the constraint of the ALMPC is updated in the meanwhile. The online updating improves the predictive model accuracy and relaxes the stability constraint, which makes the proposed scheme

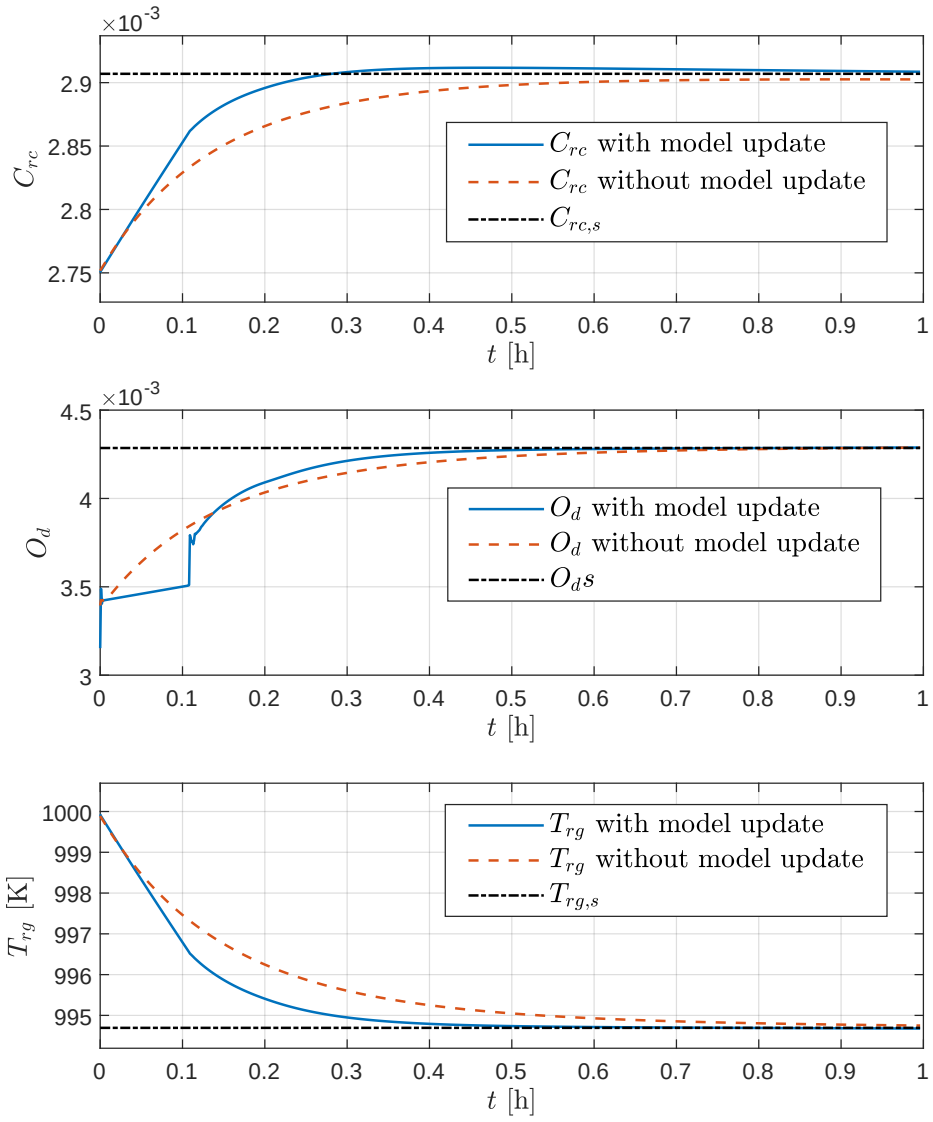


Figure 3: State trajectories of the process ($x_{sp} = [2.907 \times 10^{-3}, 4.286 \times 10^{-3}, 994.694]^T$)

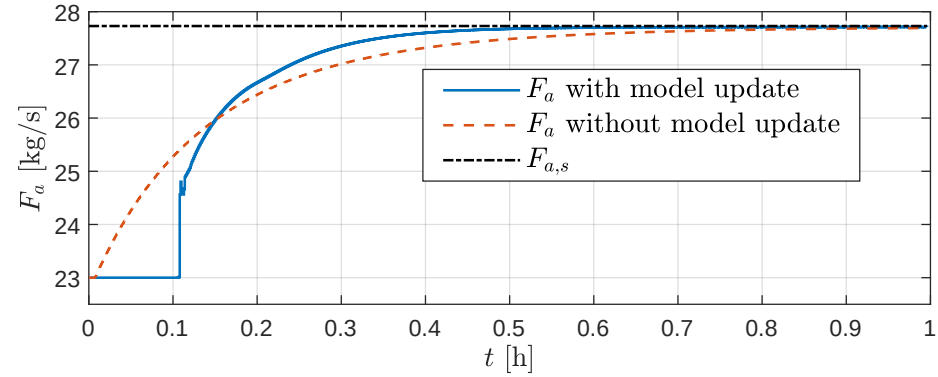


Figure 4: The manipulated input trajectories of the process

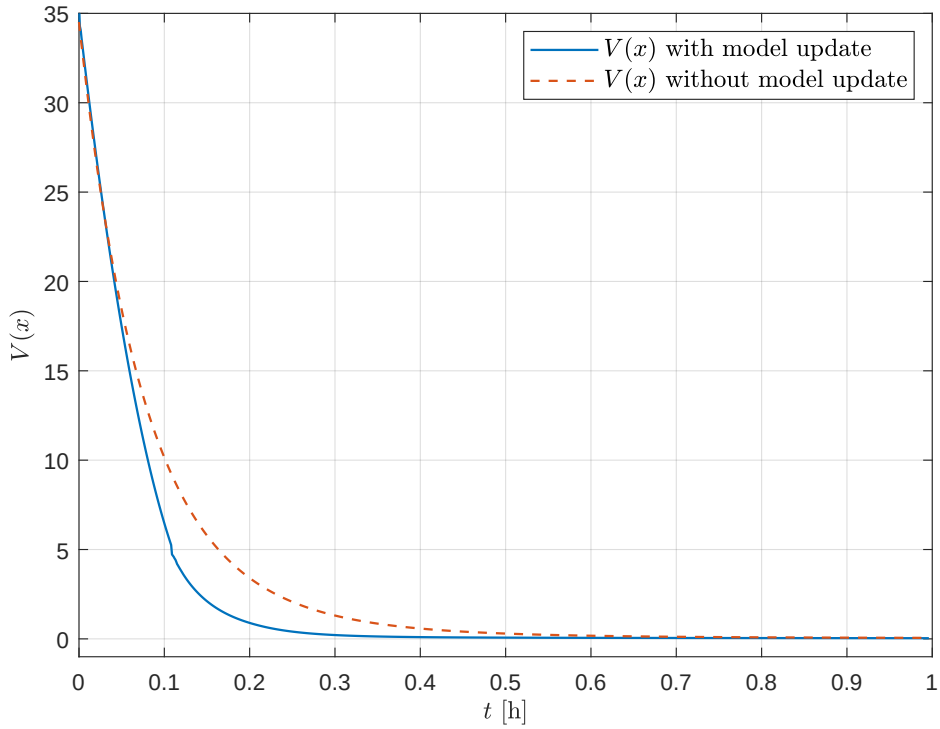


Figure 5: Lyapunov function value V(x) trajectories

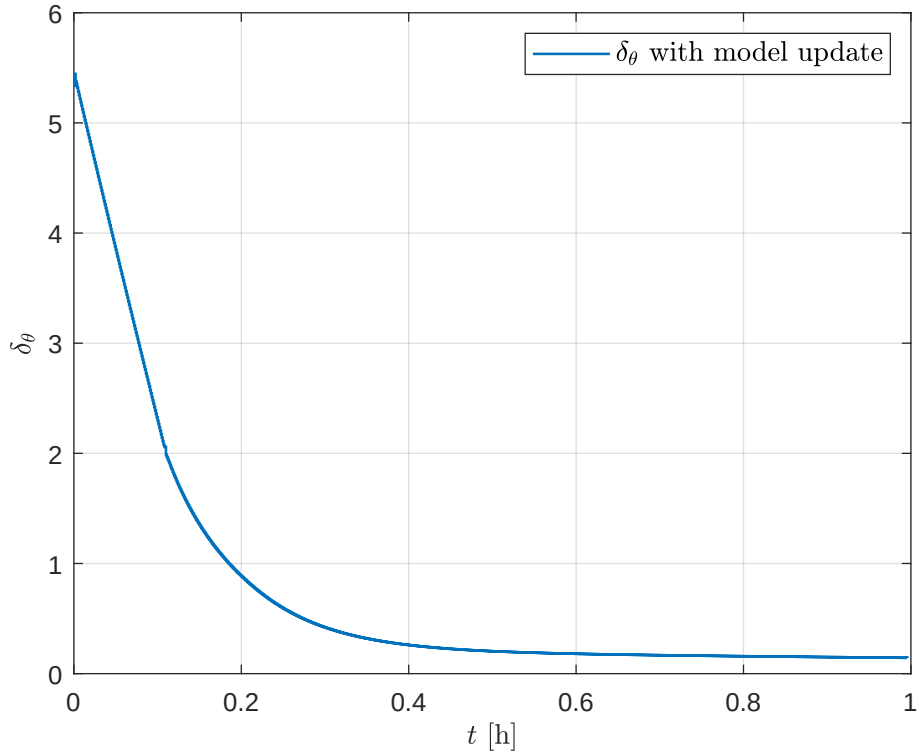


Figure 6: The trajectory of the Lipschitz constant $\delta_\theta$

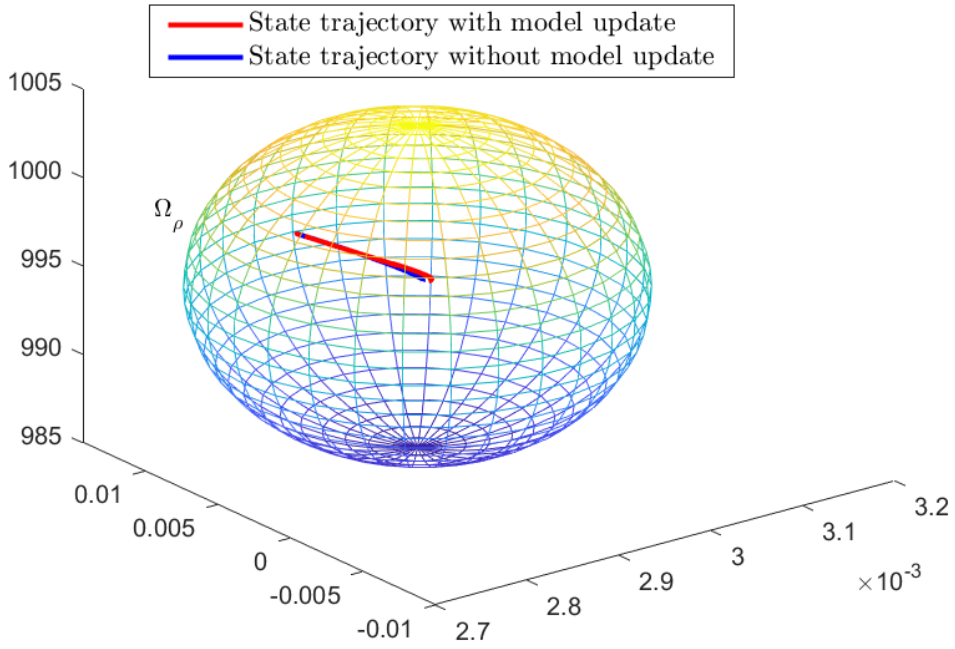


Figure 7: The 3D trajectory of the process state

a better closed-loop performance. Through this method, the states of the nonlinear system will eventually converge to a small neighborhood of the set points, and the size of the small unstable region decreases with the increasing accuracy of the linear model. Getting benefit from the linear model, the proposed method decreases the complexity of the model and improves the computational efficiency. The proposed scheme is verified according to the FCCU simulation results.

# Literature Cited


1. Scarlett Chen, Zhe Wu, David Rincon, and Panagiotis D. Christofides. Machine learning-based distributed model predictive control of nonlinear processes. *AIChE Journal*, 66(11), 2020.
2. Milan Korda and Igor Mezić. Linear predictors for nonlinear dynamical systems: Koopman operator meets model predictive control. *Automatica*, 93:149–160, 2018.
3. Z. Wu, R. Anh, D. Rincon, and P. D. Christofides. Machine learning-based predictive control of nonlinear processes. part i: Theory. *Aiche Journal*, 65(11), 2019.
4. H. Zhang, S. Li, and Y. Zheng. Q-learning-based model predictive control for nonlinear continuous-time systems. *Industrial & Engineering Chemistry Research*, 59(40):17987–17999, 2020.
5. Gang Cao, Edmund M-K Lai, and Fakhrul Alam. Gaussian process model predictive control of an unmanned quadrotor. *Journal of Intelligent & Robotic Systems*, 88(1):147–162, 2017.

6. Michael Maiworm, Daniel Limon, and Rolf Findeisen. Online learning-based model predictive control with gaussian process models and stability guarantees. *International Journal of Robust and Nonlinear Control*, 2021.
7. Yi Zheng, Tongqiang Zhang, Shaoyuan Li, Guanlin Zhang, and Yanye Wang. Gp-based mpc with updating tube for safety control of unknown system. *Digital Chemical Engineering*, 4:100041, 2022.
8. Zhe Wu, David Rincon, and Panagiotis D. Christofides. Real-time adaptive machine-learning-based predictive control of nonlinear processes. *Industrial & Engineering Chemistry Research*, 59(6):2275–2290, 2019.
9. Anil Aswani, Humberto Gonzalez, S Shankar Sastry, and Claire Tomlin. Provably safe and robust learning-based model predictive control. *Automatica*, 49(5):1216–1226, 2013.
10. Zhe Wu, Aisha Alnajdi, Quanquan Gu, and Panagiotis D Christofides. Statistical machine-learning–based predictive control of uncertain nonlinear processes. *AIChE Journal*, 68(5):e17642, 2022.
11. T. Zhang, S Li, Y. Zheng, and Y Wang. Implementable stability guaranteed lyapunov-based data-driven model predictive control with evolving gaussian process. *Industrial Engineering & Chemical Research*, 23(9):1306–1319, 2022.
12. Eric Bradford, Lars Imsland, Dongda Zhang, and Ehecatl Antonio del Rio Chanona. Stochastic data-driven model predictive control using gaussian processes. *Computers & Chemical Engineering*, 139:106844, 2020.
13. Xin Xu, Hong Chen, Chuanqiang Lian, and Dazi Li. Learning-based predictive control for discrete-time nonlinear systems with stochastic disturbances. *IEEE transactions on neural networks and learning systems*, 29(12):6202–6213, 2018.
14. Jinfeng Liu, David Muñoz de la Peña, and Panagiotis D. Christofides. Distributed model predictive control of nonlinear systems subject to asynchronous and delayed measurements. *Automatica*, 46(1):52–61, 2010.
15. Mohsen Heidarinejad, Jinfeng Liu, and Panagiotis D. Christofides. Economic model predictive control of nonlinear process systems using lyapunov techniques. *AIChE Journal*, 58(3):855–870, 2012.
16. Y. Zheng, S. Y. Li, R. X. Wan, and Y. Y. Wang. Economic lyapunov-based model predictive control with event-triggered parametric identification. *International Journal of Robust and Nonlinear Control*, 32(1):205–226, 2022.
17. Veronica Adetola, Darryl DeHaan, and Martin Guay. Adaptive model predictive control for constrained nonlinear systems. *Systems & Control Letters*, 58(5):320–326, 2009.

18. Gaa Gon Alves and M. Guay. Robust discrete-time set-based adaptive predictive control for nonlinear systems. *Journal of Process Control*, 39:111–122, 2016.
19. B. O. Koopman. Hamiltonian systems and transformation in hilbert space. *Proceedings of the National Academy of Sciences*, 17(5):315–318, 1931.
20. Torsten Carleman. Application de la théorie des équations intégrales linéaires aux systèmes d'équations différentielles non linéaires. *Acta Mathematica*, 59(none):63 – 87, 1932.
21. Matthew O. Williams, Ioannis G. Kevrekidis, and Clarence W. Rowley. A data-driven approximation of the koopman operator: Extending dynamic mode decomposition. *Journal of Nonlinear Science*, 25(6):1307–1346, 2015.
22. M. Budisic, R. Mohr, and I. Mezic. Applied koopmanism. *Chaos*, 22(4):047510, 2012.
23. Zlatko Drmač, Igor Mezić, and Ryan Mohr. Identification of nonlinear systems using the infinitesimal generator of the koopman semigroup—a numerical implementation of the mauroy–goncalves method. *Mathematics*, 9(17), 2021.
24. Alexandre Mauroy and Jorge Goncalves. Koopman-based lifting techniques for nonlinear systems identification. *IEEE Transactions on Automatic Control*, 65(6):2550–2565, June 2020.
25. M. Lorenzen, M. Cannon, and F Allgöwer. Robust mpc with recursive model update. *Automatica*, 103:461–471, 2019.
26. Derui Ding, Zidong Wang, and Qing-Long Han. A set-membership approach to event-triggered filtering for general nonlinear systems over sensor networks. *IEEE Transactions on Automatic Control*, 65(4):1792–1799, 2019.
27. E. W. Bai, H. Cho, and R. Tempo. Convergence properties of the membership set. *Automatica*, 34(10):1245–1249, 1998.
28. Eduardo D Sontag. A 'universal' construction of artstein's theorem on nonlinear stabilization. *Systems & control letters*, 13(2):117–123, 1989.
29. Eli Fogel and Yih-Fang Huang. On the value of information in system identification—bounded noise case. *Automatica*, 18(2):229–238, 1982.
30. John R Deller, Majid Nayeri, and Souheil F Odeh. Least-square identification with error bounds for real-time signal processing and control. *Proceedings of the IEEE*, 81(6):815–849, 1993.
31. M. Hovd and S. Skogestad. Procedure for regulatory control structure selection with application to the fcc process. *AIChE Journal*, 39(12):1938–1953, 1993.